Surface polaritons of small coated cylinders illuminated by normal incident TM and TE plane waves

Hao-Yuan She and Le-Wei Li

Nanoscience & Nanotechnology Initiative and Dept of Electrical & Computer Engineering
National University of Singapore, Kent Ridge, Singapore 119260

lwli@nus.edu.sg

Olivier J.F. Martin and Juan R. Mosig

Institut de Transmissions, Ondes et Photonique (ITOP)
Swiss Federal Institute of Technology in Lausanne (EPFL), Switzerland

olivier.martin@epfl.ch

juan.mosig@epfl.ch

Abstract: The surface polariton properties of TM or TE plane wave scattered by a coated cylinder are investigated in this paper. The coated cylinder (whose outer radius is much smaller than the wavelength) is assumed to be electrically small and low dissipative. Analytical formulas of the plasmonic resonances are derived and found to agree well with those obtained from exact expressions in the classical scattering theory. The behaviors of the scattering coefficients at resonances are also discussed and compared for different cases. While a single cylinder has the resonance at the relative permittivity of $\varepsilon_r = -1$ (or relative permeability of $\mu_r = -1$) for the TE (or TM) polarization, the resonances of the coated cylinders change with different n values (where n denotes the series term or mode of the field), and also the inner and outer radii. It is shown that the scattered field in the near zone can be enhanced significantly compared to the incident wave. For the TE incident case, we take a silver coated nano-cylinder as an example to illuminate the near-field optical effect. Also, we have studied the peak values of the nth order scattered field for different n values and electrical parameter $k_0 b$ (where k_0 is the wavenumber of the free space and b denotes the outer radius of the cylinder) around the cylinder. The derived new formulas for total cross sections are given and they may provide us with some potential photonic applications such as surface cleaning and etching.

OCIS codes: (160.3918) Metamaterials; (160.4760) Optical properties; (240.0240) Physical optics; (240.5420) Polaritons; (240.6680) Surface plasmons.

References and links

1. V. G. Veselago, "The electrodynamics of substances with simultaneously negative values of ε and μ," Sov. Phys. Usp. **10**, 509-514 (1968).
2. R. A. Shelby, D. R. Smith, and S. Schultz, "Experimental verification of a negative index of refraction," Science, **292**, 77-79 (2001).

#89185 - $15.00 USD Received 27 Nov 2007; revised 31 Dec 2007; accepted 4 Jan 2008; published 11 Jan 2008

3. N. Feth, C. Enkrich, M. Wegener, and S. Linden, "Large-area magnetic metamaterials via compact interference lithography," Opt. Express **15**, 501-507 (2007).
4. C. Rockstuhl, F. Lederer, C. Etrich, Th. Zentgraf, J. Kuhl, and H. Giessen, "On the reinterpretation of resonances in split-ring-resonators at normal incidence," Opt. Express **14**, 8827-8836 (2006).
5. S. Zhang, W. Fan, K. J. Malloy, S. R. J. Brueck, N. C. Panoiu and R. M. Osgood, "Near-infrared double negative metamaterials," Opt. Express **13**, 4922-4930 (2005).
6. Z. Ku and S. R. J. Brueck, "Comparison of negative refractive index materials with circular, elliptical and rectangular holes," Opt. Express **15**, 4515-4522 (2007).
7. L. W. Li, W. Xu, H. Y. Yao, Z. N. Chen, and Q. Wu, "Design of left-handed metamaterials using single resonant and double resonant structures," Int'l J. Microwave Opt. Tech. **1**, 10-16 (2006).
8. C. W. Qiu, H. Y. Yao, L. W. Li, S. Zouhdi, and T. S. Yeo, "Backward waves in magnetoelectrically chiral media: propagation, impedance, and negative refraction", Phys. Rev. B **75**, 155120 (1-7) (2007).
9. C. W. Qiu, H. Y. Yao, L. W. Li, S. Zouhdi, and T. S. Yeo, "Routes to left-handed materials by magnetoelectric couplings", Phys. Rev. B **75**, 245214 (1-7) (2007).
10. Q. Cheng and T. J. Cui, "Negative refractions and backward waves in biaxially anisotropic chiral media," Opt. Express **14**, 6322-6332 (2006).
11. A. Cho, "Voilà! Cloak of invisibility unveiled," Science **314**, 403 (2006).
12. Y. Huang, Y. Feng, and T. Jiang, "Electromagnetic cloaking by layered structure of homogeneous isotropic materials," Opt. Express **15**, 11133-11141 (2007).
13. A. Greenleaf, Y. Kurylev, M. Lassas, and G. Uhlmann, "Improvement of cylindrical cloaking with the SHS lining," Opt. Express, **15**, 12717-12734 (2007).
14. H. Y. Yao, L. W. Li, C. W. Qiu, Q. Wu, and Z. N. Chen, "Properties of electromagnetic waves in a multilayered cylinder filled with double negative and positive materials," Radio Sci. **42**, 2006RS003509 (1-8) (2007).
15. S. Ancey, Y. Decanini, A. Folacci and P. Gabrielli, "Surface polaritons on left-handed cylinders: a complex angular momentum analysis," Phys. Rev. B **72**, 085458 (1-18) (2005).
16. R. Ruppin, "Surface polaritons and extinction properties of a left-handed material cylinder," J. Phys.: Condens. Matter **16**, 5991-5998 (2004).
17. M. A. Mushref, "Closed solution to electromagnetic scattering of a plane wave by an eccentric cylinder coated with metamaterials," Opt. Commun. **270**, 441-446 (2007).
18. H. Vollmer and E. J. Rothwell,"Resonance series representation of the early-time field scattered by a coated cylinder," IEEE Trans. Antennas Propag. **52**, 2186-2190 (2004).
19. B. S. Luk'yanchuk and V. Ternovsky, "Light scattering by a thin wire with a surface-plasmon resonance: bifurcations of the Poynting vector field," Phys. Rev. B **73**, 235432 (1-12) (2006).
20. S. Arslanagic, R. W. Ziolkowski, and O. Breinbjerg, "Excitation of an electrically small metamaterial-coated cylinder by an arbitrarily located line source," Microwave Opt. Tech. Lett. **48**, 2598-2605 (2006).
21. C. C. H. Tang, "Backscattering from dielectric-coated infinite cylindrical obstacles," J. Appl. Phys. **28**, 628-633 (1957).
22. P. B. Johnson and R. W. Christy, "Optical constants of the noble metals," Phys. Rev. B **6**, 4370-4379 (1972).
23. H. S. Chu, W. B. Ewe, E. P. Li, and R. Vahldieck, "Analysis of sub-wavelength light propagation through long double-chain nanowires with funnel feeding," Opt. Express **15**, 4216-4223 (2007).
24. U. Schröster and A. Dereux, "Surface plasmon polaritons on metal cylinders with dielectric core," Phys. Rev. B **64**, 125420 (1-10) (2001).

1. Introduction

In the past several years, negative index materials or metamaterials, which were proposed using split-ring resonator (SRR) structures and found to exhibit negative refractive index (NRI) characteristics [1], attracted considerable attentions [2]. Properties exhibited by metamaterials have also been discussed thoroughly from design to potential applications [3–10]. Recently, the invisible cloaking in microwave frequency [11–13] was reported and its physical realization is now moved from microwave frequencies to visible optical frequencies. Along this line, properties of light scattering by metamaterial objects are apparently very important and essential in the further investigations and characterizations.

Scattering of light by metamaterial cylinders is also of recent interests and has been widely discussed [14]. The surface polaritons can be seen from the resulted cross sections versus ω/ω_p. Surface polaritons on left-handed material cylinders were discussed thoroughly in [15] and [16]. It is found that the electrostatic and magnetostatic resonances occur respectively at $\varepsilon_r = -1$ (for the TE wave incidence) or $\mu_r = -1$ (for the TM wave incidence). Mushref provided the closed-

#89185 - $15.00 USD Received 27 Nov 2007; revised 31 Dec 2007; accepted 4 Jan 2008; published 11 Jan 2008

form solution to electromagnetic scattering of a plane wave by an eccentric cylinder coated with metamaterials [17]. The transient response of a coated cylinder to a plane-wave excitation was reported by Vollmer and Rothwell [18]. It is shown that the plasmonic cylinders can be exited only by TE plane wave [19]. The plasmon resonance is found to occur near $\Re\mathrm{e}(\varepsilon_r) = -1$ (where $\varepsilon_r = \varepsilon' + i\varepsilon''$ denotes the relative permittivity of the cylinder) for two dimensional electrically small cylinders [19].

Arslanagic *et al.* studied an electrically small metamaterial-coated cylinder excited by an arbitrarily located line source [20]. The backscattering properties of dielectric-coated cylindrical structures were discussed in [21]. Johnson and Christy measured the optical constants of noble metals (copper, silver, and gold) in the spectral range 0.5-6.5 eV with an oblique-incidence thin-film technique [22]. The transmission properties of light in two dimensional structures were investigated in [23]. Surface plasmon polaritons of different orders on metal cylinders with dielectric core were studied in [24].

In this paper, we will further look into the problems of a coated cylinder scattered by TM and TE plane waves. The focus of this paper is to investigate analytically the plasmonic resonance characteristics and peculiarities of light scattering by a coated-cylinder of electrically small radius, where the metamaterial is considered as either the core or the coating material in the scattering system.

2. Theoretical foundation

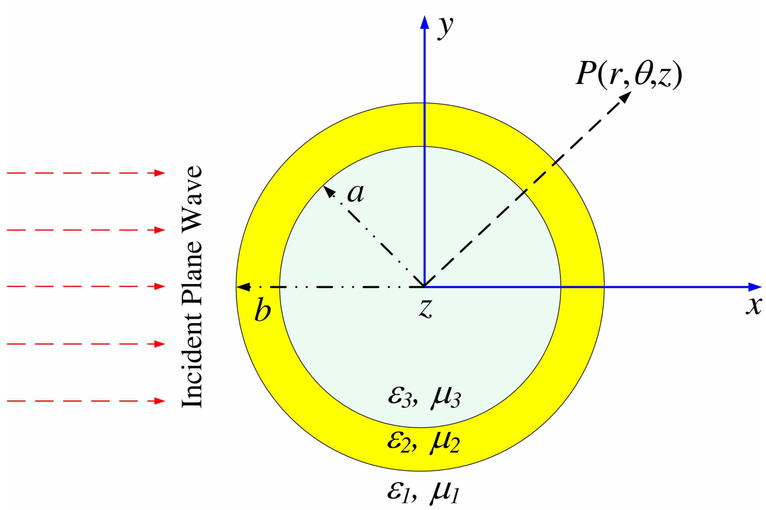

Fig. 1. Geometry for scattering of a plane wave by a coated cylinder.

The geometry of the problem is shown in Fig. 1. The incident wave is a TM plane wave whose electric field is polarized in the z-direction (along the axis of the cylinder) and can be expressed as in [21] by

$$E_z^{\mathrm{inc}} = E_1^i = E_0 \sum_{n=-\infty}^{\infty} i^n J_n(k_1\rho) e^{in\theta}. \tag{1}$$

Therefore, the scattered field in the outer region consisting of the out-going waves must be of the form

$$E_1^{\mathrm{sc}} = E_0 \sum_{n=-\infty}^{\infty} i^n A_n H_n^{(1)}(k_1\rho) e^{in\theta}; \tag{2a}$$

#89185 - $15.00 USD Received 27 Nov 2007; revised 31 Dec 2007; accepted 4 Jan 2008; published 11 Jan 2008

while the electric field in the coating region consisting of the out-going and in-coming waves is given by

$$E_2 = E_0 \sum_{n=-\infty}^{\infty} i^n \left[B_n H_n^{(2)}(k_2\rho) + C_n H_n^{(1)}(k_2\rho) \right] e^{in\theta}; \tag{2b}$$

and the transmitted field in the core consisting of the standing wave can be written as

$$E_3 = E_0 \sum_{n=-\infty}^{\infty} i^n D_n J_n(k_3\rho) e^{in\theta} \tag{2c}$$

where $J_n(\bullet)$ stands for the cylindrical Bessel function of the first kind and the order n, $H_n^{(1)}(\bullet)$ and $H_n^{(2)}(\bullet)$ represent the cylindrical Hankel functions of the first and second kinds and the order n, respectively, θ denotes the angle shown in Fig. 1, g identifies the observation point, k_1, k_2 and k_3 are the wavenumbers in free space, the coating region and the core region, respectively, and ε_i and μ_i ($i = 1$, 2, and 3) denote the relative permittivities and permeabilities of the three regions. We let $p = k_0a$ and $q = k_0b$ which denote the electrical dimension of the inner and outer radii. When the boundary conditions at $\rho = a$ and $\rho = b$ (where a and b denote the inner and outer radii of the coated cylinder, respectively) are applied, we can obtain the following equations

$$\begin{aligned}
H_n^{(1)}(k_1b)A_n - H_n^{(2)}(k_2b)B_n - H_n^{(1)}(k_2b)C_n &= -J_n(k_1b), && \text{(3a)}\\
H_n^{(2)}(k_2a)B_n + H_n^{(1)}(k_2a)C_n - J_n(k_3a)D_n &= 0, && \text{(3b)}\\
\frac{k_1}{\mu_1}H_n^{'(1)}(k_1b)A_n - \frac{k_2}{\mu_2}H_n^{'(2)}(k_2b)B_n - \frac{k_2}{\mu_2}H_n^{'(1)}(k_2b)C_n &= -\frac{k_1}{\mu_1}J_n'(k_1b), && \text{(3c)}\\
\frac{k_2}{\mu_2}H_n^{'(2)}(k_2a)B_n + \frac{k_2}{\mu_2}H_n^{'(1)}(k_2a)C_n - \frac{k_3}{\mu_3}J_n'(k_3a)D_n &= 0, && \text{(3d)}
\end{aligned}$$

where the prime denotes the derivative with respect to the argument. Now we are able to obtain the scattering coefficient A_n of special interest in this paper and the other coefficients B_n, C_n, and D_n of no interest in this paper. The coefficient A_n is given below:

$$A_n = \frac{\frac{\mu_2}{\mu_1}J_n'(k_1b)\left[H_n^{(2)}(k_2b)P_n + H_n^{(1)}(k_2b)\right] - \frac{k_2}{k_1}J_n(k_1b)\left[H_n^{'(2)}(k_2b)P_n + H_n^{'(1)}(k_2b)\right]}{\frac{k_2}{k_1}H_n^{(1)}(k_1b)\left[H_n^{'(2)}(k_2b)P_n + H_n^{'(1)}(k_2b)\right] - \frac{\mu_2}{\mu_1}H_n^{'(1)}(k_1b)\left[H_n^{(2)}(k_2b)P_n + H_n^{(1)}(k_2b)\right]} \tag{4}$$

where

$$P_n = \frac{\frac{\mu_3}{\mu_2}J_n(k_3a)H_n^{'(1)}(k_2a) - \frac{k_3}{k_2}J_n'(k_3a)H_n^{(1)}(k_2a)}{\frac{k_3}{k_2}J_n'(k_3a)H_n^{(2)}(k_2a) - \frac{\mu_3}{\mu_2}J_n(k_3a)H_n^{'(2)}(k_2a)}. \tag{5}$$

As the other coefficients are not of our interest in this paper, thus they will not be provided herein. The coefficient provided here is explicitly expressed and it is exact in accuracy. The total scattering cross section is defined as the ratio of the total power scattered to the incident power per unit length and is given by

$$\sigma_{\text{total}} = \frac{4}{k_1}\sum_{n=-\infty}^{\infty} |A_n|^2. \tag{6}$$

From the total cross section expression, the surface modes can be thus obtained using the numerically exact solution to the above expression, but the solution is implicit in expression. To

#89185 - $15.00 USD Received 27 Nov 2007; revised 31 Dec 2007; accepted 4 Jan 2008; published 11 Jan 2008

gain more physical insight into the modes and also the relationships among the parameters, we will subsequently try to obtain them explicitly.

From the subsequent approximate but explicit formulations, it is clearly seen that the multiple resonances can be obtained in the following cases.

- The surface modes will occur for a given summation index n or a fixed single mode in Eqn. (6); and the maximum intensity of scattered field at resonances decreases continuously versus the outer radius b.
- The surface modes will occur for different summation indices $n = 1, 2, 3, \cdots$ or their various multiple modes; and the resonance for each of the modes can be the same in magnitude and can reach unity although the bandwidth of such a resonance decreases drastically with the order n of the modes.
- In addition to the multiple modes, the multiple resonances are a function of the physical parameters a and b of the coated cylinder. While the maximum magnitude at its resonance is fixed at unity, the bandwidth varies with a and b.

When the argument $|z| \ll 1$, we can use, for $n > 0$, the following approximations of the Bessel and Hankel functions

$$J_n(z) \approx \frac{(0.5z)^n}{\Gamma(n+1)}, \tag{7a}$$

$$H_n^{(1)}(z) \approx \frac{(0.5z)^n}{\Gamma(n+1)} - i\frac{\Gamma(n)}{\pi}\left(\frac{2}{z}\right)^n, \tag{7b}$$

$$H_n^{(2)}(z) \approx \frac{(0.5z)^n}{\Gamma(n+1)} + i\frac{\Gamma(n)}{\pi}\left(\frac{2}{z}\right)^n, \tag{7c}$$

where Γ denotes the Gamma function. For $n < 0$, the approximations are similar to those of $n > 0$, and will not be discussed here. Substituting the approximate formulas into A_n and omitting the higher order terms, we have

$$A_n \simeq -\frac{i\pi\left(\frac{k_1 b}{2}\right)^{2n}\left[\left(\frac{a}{b}\right)^{2n}(\mu_1+\mu_2)(\mu_2-\mu_3)+(\mu_1-\mu_2)(\mu_2+\mu_3)\right]}{\Gamma(n)\Gamma(n+1)\left[\left(\frac{a}{b}\right)^{2n}(\mu_1-\mu_2)(\mu_2-\mu_3)+(\mu_1+\mu_2)(\mu_2+\mu_3)\right]}. \tag{8}$$

By enforcing the denominator, when $n \neq 0$, to be zero, we can obtain the resonances. As a result, we come up with the following equation in free space:

$$\left(\frac{a}{b}\right)^{2n}(\mu_1-\mu_2)(\mu_2-\mu_3)+(\mu_1+\mu_2)(\mu_2+\mu_3) = 0. \tag{9}$$

When Eqn. (9) is satisfied, we can find the surface modes of metamaterial-coated cylinders. It is apparent that for metamaterial-core cylinders, there exists only one mode; but for metamaterial-coated cylinders, two modes can be found to exist simultaneously. In addition, we would indicate from Eqn. (9) that the resonance depends on not only the surrounding medium, but also the physical diameters (in the present case, the ratio of radius a to radius b). It should also be noted that for $n = 0$, A_0 will have no resonances. And for $n < 0$, $A_n = A_{-n}$ which means that A_{-n} has the same resonances as A_n.

The surface modes can be obtained directly using the exact expression in Eqn. (6) for the coefficients of multiple orders, and it can be also obtained from the above asymptotic formula

#89185 - $15.00 USD Received 27 Nov 2007; revised 31 Dec 2007; accepted 4 Jan 2008; published 11 Jan 2008

in Eqn. (9). Through a few numerical examples, we found that the above solutions obtained using the approximate approach are fairly accurate as compared to the exact solutions; so a detailed comparison will not be shown here.

When the incident wave is TE plane wave, the corresponding items need to be modified. The electric field should be replaced by magnetic field and some changes in the boundary conditions should be made. In this case, we can obtain, after solving the equations and simplifying the scattering coefficient, the equation from the denominator of the scattering coefficient:

$$\left(\frac{a}{b}\right)^{2n}(\varepsilon_1-\varepsilon_2)(\varepsilon_2-\varepsilon_3)+(\varepsilon_1+\varepsilon_2)(\varepsilon_2+\varepsilon_3)=0. \tag{10}$$

By comparing Eqn. (9) with Eqn. (10), it can be easily seen that the two solutions are reciprocal and they can be obtained one from the other simply by replacing μ by ε or its vice versa. Subsequently, we will discuss the characteristics of the two (TM and TE) modes.

3. Coated cylinders scattered by TM plane wave

From Eqn. (9), we can find two resonances of coated cylinders with metamaterial coating. To mathematically describe them, we write the roots in the form of

$$\mu_2=\frac{G\pm H}{F} \tag{11}$$

where

$$G = -\left[\mu_1+\left(\frac{a}{b}\right)^{2n}\mu_1+\mu_3+\left(\frac{a}{b}\right)^{2n}\mu_3\right], \tag{12a}$$

$$H = \sqrt{\left[\mu_1+\left(\frac{a}{b}\right)^{2n}\mu_1+\mu_3+\left(\frac{a}{b}\right)^{2n}\mu_3\right]^2-4\mu_1\mu_3\left[\left(\frac{a}{b}\right)^{2n}-1\right]^2}, \tag{12b}$$

$$F = 2\left[1-\left(\frac{a}{b}\right)^{2n}\right]. \tag{12c}$$

When the metamaterial core cylinder is coated with positive index material, thus $\mu_3<0$ and $\mu_2>0$. Then solving the characteristic equation Eqn. (9), we can obtain

$$\mu_3=-\mu_2\frac{\mu_1+\left(\frac{a}{b}\right)^{2n}\mu_1+\mu_2-\left(\frac{a}{b}\right)^{2n}\mu_2}{\mu_1-\left(\frac{a}{b}\right)^{2n}\mu_1+\mu_2+\left(\frac{a}{b}\right)^{2n}\mu_2} \tag{13}$$

which represents the surface modes of the cylinder. It is apparent that the surface modes of a light scattered by a coated cylinder are much more complicated than that (*i.e.*, only one surface mode when $\varepsilon_r=-1$ or $\mu_r=-1$) of a single cylinder [15].

It should be pointed that in the subsequent derivations of the resonances, we have used the exact solution for all the cases. However, we also provide the small-argument approximation to gain more physical modes or insights and to obtain the approximate locations of the resonances. When the damping is moderately large, the small argument solution is found to be still accurate enough, as compared to the exact solution. When the damping is small or zero (lossless), then the exact solution must be used to derive the resonances [19].

#89185 - $15.00 USD Received 27 Nov 2007; revised 31 Dec 2007; accepted 4 Jan 2008; published 11 Jan 2008

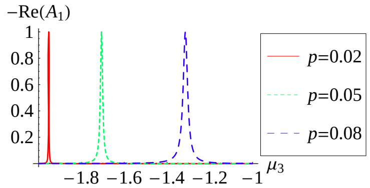

(a) $q = 0.1$ and $\mu_2 = 2$

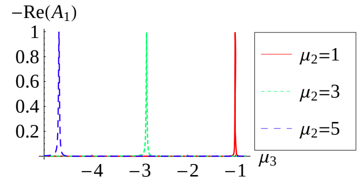

(b) $q = 0.2$ and $p = 0.05$

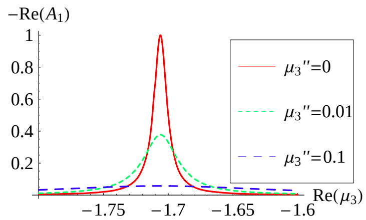

(c) $q = 0.1$ and $p = 0.05$

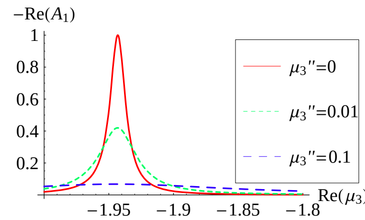

(d) $q = 0.2$ and $p = 0.05$

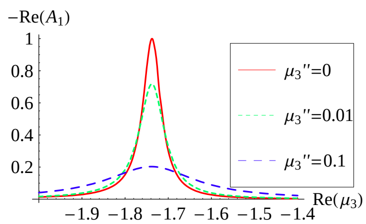

(e) $q = 0.2$ and $p = 0.1$

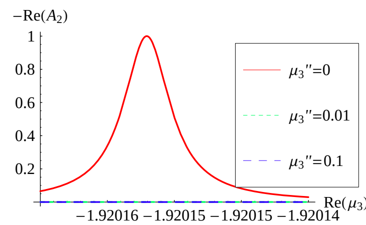

(f) $q = 0.1$ and $p = 0.05$

Fig. 2. Variation of the scattering coefficient A_n with various parameters.

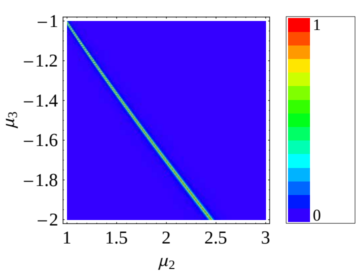

(a) $q = 0.1$ and $p = 0.05$

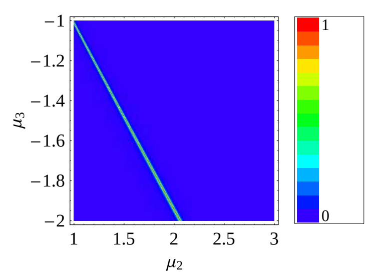

(b) $q = 0.2$ and $p = 0.05$

Fig. 3. The density plot of $-\Re\mathrm{e}(A_1)$ versus μ_2 and μ_3.

3.1. *Coated cylinders with metamaterial cores*

The $-\Re\mathrm{e}(A_1)$ values versus μ_3 are now obtained (firstly, we consider the lossless cases) and plotted in Fig. 2(a) and Fig. 2(b) for different values of $q = k_0 b$ and μ_2. It is seen in Fig. 2(a) that with increase of the inner radius a or the electrical size $p = k_0 a$, the μ_3 values at resonances become smaller. It is clearly seen that all values of $-\Re\mathrm{e}(A_1)$ at resonances can reach their peaks of 1, which is the same as light scattering by a single plasmonic cylinder. We can also see in Fig. 2(b) that when q is increased to 0.2 and $p = 0.05$, the values of μ_3 at resonances will decrease accordingly with the increase of μ_2. The absolute values of μ_3 at resonances

#89185 - $15.00 USD Received 27 Nov 2007; revised 31 Dec 2007; accepted 4 Jan 2008; published 11 Jan 2008

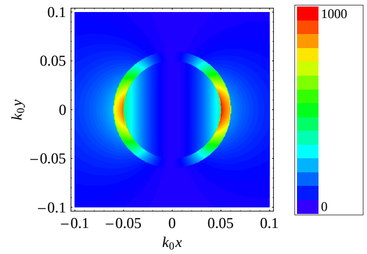

(a) $q = 0.06$, $p = 0.05$ and $\mu_3 = -1.26$

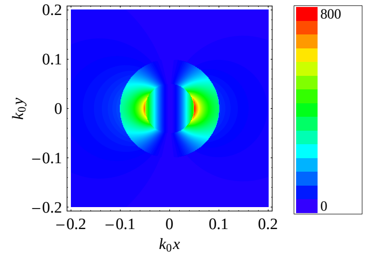

(b) $q = 0.1$, $p = 0.05$ and $\mu_3 = -1.7$

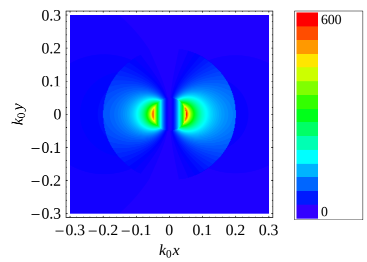

(c) $q = 0.2$, $p = 0.05$ and $\mu_3 = -1.95$

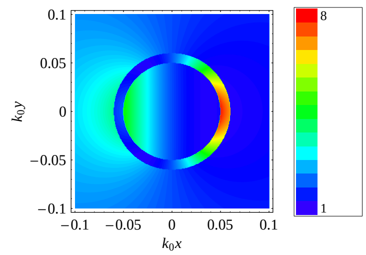

(d) $q = 0.06$, $p = 0.05$ and $\mu_3 = -1.26 + 0.1i$

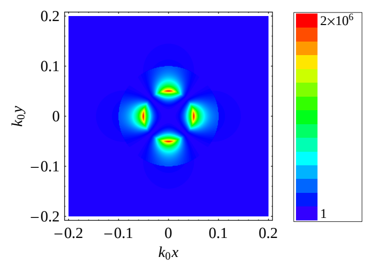

(e) $q = 0.1$, $p = 0.05$ and $\mu_3 = -1.92\ldots$

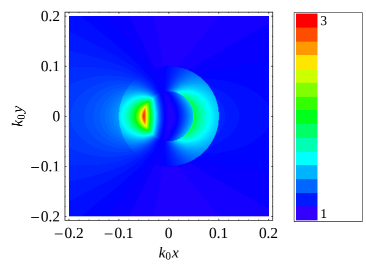

(f) $q = 0.1$, $p = 0.05$ and $\mu_3 = -1.92\ldots + 0.01i$

Fig. 4. The energy distributions of the coated cylinder near resonances.

are very close to μ_2. When the damping term is taken into consideration, $-\Re e(A_1)$ values are again plotted for different size parameters of p and q in Figs. 2(c)-(e). It is observed that even with some very small dissipation, the scattering coefficients at resonances can be significantly reduced in value. One can also see the changes in the bandwidth and peak values of $-\Re e(A_1)$ affected by μ_3''. For different μ_3'' values, the positions of the resonances do not vary.

For solutions of the higher orders, we take $n = 2$ as an example; and $-\Re e(A_2)$ values are shown in Fig. 2(f). Without dissipation, the $-\Re e(A_2)$ can also reach its maximum of 1. A very small value of μ_3'' can lead, however, significant reduction of $-\Re e(A_2)$ and the other higher-order coefficients. This also explains why the higher orders are not interested in reality. The dissipation has a greater effect on the higher modes than the lower ones.

The density plots of $-\Re e(A_1)$ versus μ_2 and μ_3 are shown in Fig. 3(a) and Fig. 3(b) for different values of $q = 0.1$ and $q = 0.2$ (where $q = k_0 b$ denotes the electrical dimension of the outer radius), when p is chosen to be $p = 0.05$. The resonance traces for both cases are clearly observed from the contours of $-\Re e(A_1)$. From these figures, the relationships between μ_2 and μ_3 at resonances are clearly depicted. The scale that we used in Fig. 3 is linear, and so are the

#89185 - $15.00 USD Received 27 Nov 2007; revised 31 Dec 2007; accepted 4 Jan 2008; published 11 Jan 2008

subsequent figures.

The near-field energy intensity distributions near resonances are also obtained and plotted in Fig. 4. The intensity is defined as $I = \mathbf{E} \cdot \mathbf{E}^{\star}$ where $\mathbf{E}^{\star}$ stands for the conjugate of $\mathbf{E}$. For all figures shown in Fig. 4, we let $\mu_2 = \varepsilon_2 = 2$ and $\varepsilon_3 = -2$. The relative permittivities of μ_3 are given in the figures. We assume p to be fixed at 0.05 and let q vary from 0.06, via 0.1 to 0.2. We can see that the energy in the coating region reaches the highest. We can also see that in all the three cases, the scattered near-field energies can be enhanced which is because of the increment of the scattering coefficients.

With larger values of q, however, the scattered fields become smaller relatively. This phenomenon will be further discussed later. In Fig. 4(d), the resonance of a coated cylinder is shown. The near-field energy can be still enhanced although it becomes much smaller in value than that shown in Fig. 4(a). The energy distribution of a higher-order surface mode ($n = 2$) is shown in Fig. 4(e). One can see that the near-field energy intensity is increased by many times. If we take a very small damping term (*i.e.*, the imaginary part of the relative permeability due to the dissipation, $\mu_3'' = 0.01$) into consideration, however, the energy distribution becomes, as shown in Fig. 4(f), very common.

3.2. Coated cylinders with metamaterial coatings

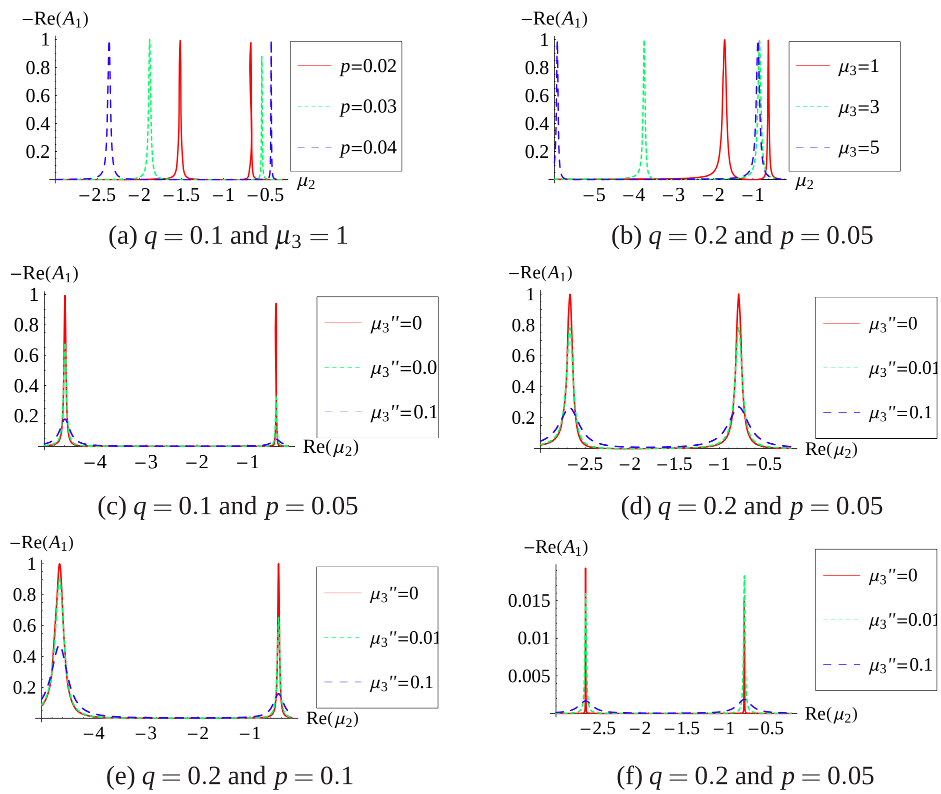

Fig. 5. $-\Re\mathrm{e}(A_1)$ versus μ_2 for different parameters.

For convenience, we label the smaller μ_2 to correspond to the first resonance and the bigger one to the second resonance. In Fig. 5, $-\Re\mathrm{e}(A_1)$ versus μ_2 is shown for different values of p and μ_3. It is clearly seen in Fig. 5(a) that for each p, there exist two resonances, one happens

#89185 - $15.00 USD Received 27 Nov 2007; revised 31 Dec 2007; accepted 4 Jan 2008; published 11 Jan 2008

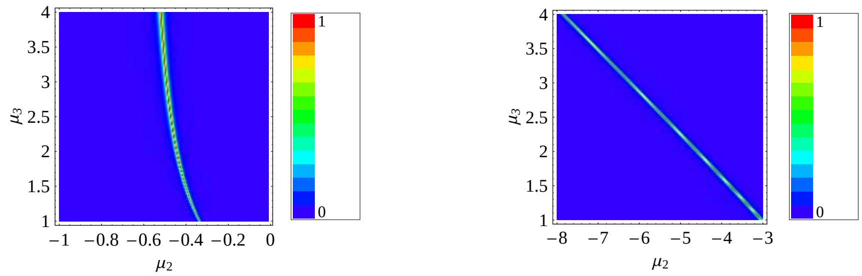

(a) The first resonance (b) The second resonance

Fig. 6. The density plot of $-\Re\mathrm{e}(A_1)$ versus μ_2 and μ_3 for the first resonance at $q = 0.1$ and $p = 0.05$.

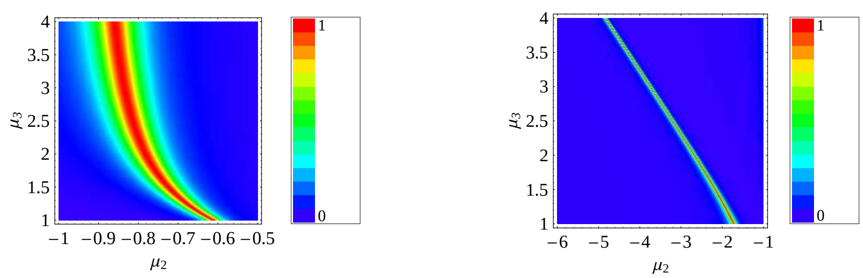

(a) The first resonance (b) The second resonance

Fig. 7. The density plot of $-\Re\mathrm{e}(A_1)$ versus μ_2 and μ_3 for the first resonance at $q = 0.2$ and $p = 0.05$.

when $\mu_2 < -1$ and the other occurs when $\mu_2 > -1$. Both resonances can reach as high as 1 at their peaks. As p becomes smaller, the two resonances become closer to each other and nearer to -1. We can see from Fig. 5(b) that for a bigger μ_3, both of the two resonances will increase in level. Also $-\Re\mathrm{e}(A_1)$ will reach its peak value of 1. This confirms our previous conclusion made below (6). The effects of μ_2'' on the properties of $-\Re\mathrm{e}(A_1)$ are shown in Fig. 5(c) to Fig. 5(f). As shown in Fig. 5(f), $-\Re\mathrm{e}(A_1)$ due to the lossless material can still reach 1 but its bandwidth is narrow, which was not discussed elsewhere.

Depicted in Fig. 6 and Fig. 7 are the distributions of $-\Re\mathrm{e}(A_1)$ versus μ_2 and μ_3. It is seen that there also exist some resonant points with different combinations of μ_2 and μ_3.

The energy intensity distributions in the near-field region near the first and second resonances are shown in Fig. 8 and Fig. 9, respectively, where we assume $\varepsilon_2 = -2$, $\varepsilon_3 = 2$ and $\mu_3 = 1$. The inner electrical radius p is fixed as 0.05 while q changes from 0.06 to 0.1. Two resonances can be seen from the energy distribution. Although we have considered only the first order mode here, the higher-order modes exhibit similar characteristics as those shown for the case of the metamaterial core. Details of the resonances and their corresponding energy intensity distributions will not be discussed herein.

#89185 - $15.00 USD Received 27 Nov 2007; revised 31 Dec 2007; accepted 4 Jan 2008; published 11 Jan 2008

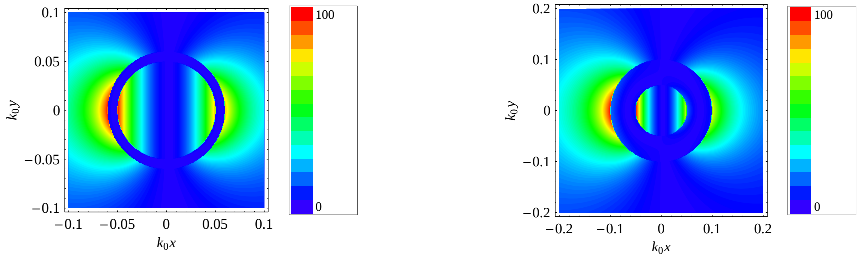

(a) $q = 0.06$, $p = 0.05$ and $\mu_2 = -0.091$ (b) $q = 0.1$, $p = 0.05$ and $\mu_2 = -0.335$

Fig. 8. The energy distributions of the coated cylinder near the first resonance.

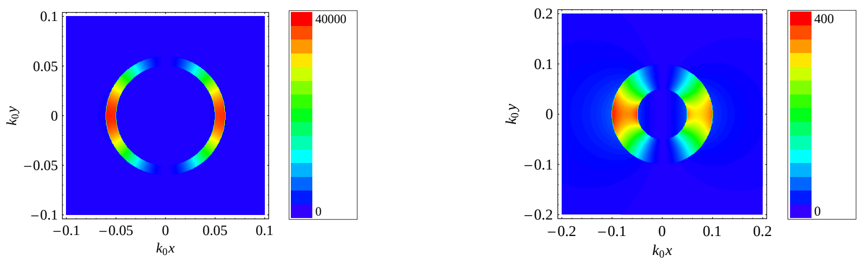

(a) $q = 0.06$, $p = 0.05$ and $\mu_2 = -11.08$ (b) $q = 0.1$, $p = 0.05$ and $\mu_2 = -3$

Fig. 9. The energy distributions of the coated cylinder near the second resonance.

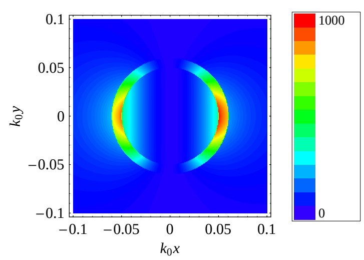

Fig. 10. The energy intensity I' distributions of a coated cylinder near resonance illuminated by TE plane wave.

4. Coated cylinders scattered by TE plane wave

For TE mode, the intensity is defined as $I' = \mathbf{H} \cdot \mathbf{H}^\star$ where $\mathbf{H}^\star$ stands for the conjugate of $\mathbf{H}$. In Fig. 10, the energy intensity surrounding a coated cylinder is plotted, where $p = 0.05$, $q = 0.06$, $\varepsilon_2 = \mu_2 = 2$, $\varepsilon_3 = -1.26$ and $\mu_3 = -2$. It is seen that the same energy intensity distribution as that shown in Fig. 4(a) is obtained. It is apparent that the magnetic field around the coated cylinder can be also enhanced. When the other parameters change, we can find the trends similar to those of the TM incident wave.

It is apparent that the plasmonic materials can also satisfy the resonance conditions because the negative relative permittivities they can produce. In Fig. 11, we plot the energy intensity

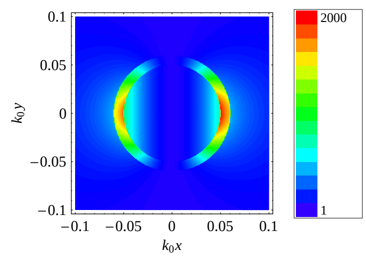

(a) $q = 0.06$ and $p = 0.05$

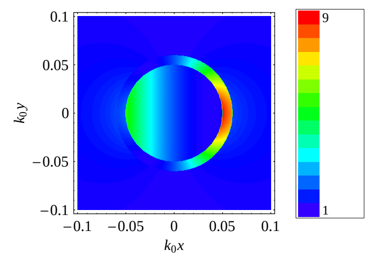

(b) $q = 0.1$ and $p = 0.05$

Fig. 11. Energy intensity of coated cylinder with or without damping term illuminated by TE plane wave.

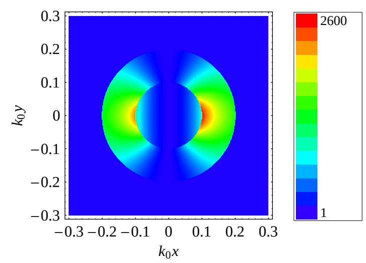

Fig. 12. Energy intensity of a silver coated nanocylinder.

of a coated cylinder with $p = 0.05$, $q = 0.06$, $\varepsilon_2 = 2$, $\mu_2 = 1$, $\varepsilon_3 = -1.26$ and $\mu_3 = 1$. As anticipated, the near-field energy intensity increases significantly. When the damping term is considered ($\varepsilon_3 = -1.26 + 0.1i$), we can see that the energy intensity drops very rapidly, as depicted in Fig. 11(b).

In Ref. 17, the optical constants of noble metals (copper, silver, and gold) are measured in the spectral range 0.5-6.5eV using an oblique incidence thin-film technique. Herein, we take the relative permittivity of silver to be $\varepsilon_3 = -27.4785 + i0.31452$ which was given in Ref. 17 at 1.64eV to see the optical properties of a silver coated nanocylinder, while the relative permittivity of coating layer is $\varepsilon_2 = 38.3$. The wavelength of the incident wave is $\lambda = 758$ nm. The outer and inner radii are 24.128 and 12.064 nm, respectively. The energy distribution is shown in Fig. 12, from which it is apparent that the near-field energy intensity can be very high for plasmonic coated nanoparticles. This is vital for some applications in surface cleaning, optical near-field etching and some others.

5. Peak values of the near-field energy intensity

How large can the scattered field be? From the previous analysis, we can see that the maximum of the scattering coefficients is $|\Re\mathrm{e}(A_n)| = 1$. The scattered field of the resonant mode is given as

$$E_1^{\mathrm{sc}} = -E_0 i^n H_n^{(1)}(k_1\rho)e^{in\theta}. \tag{14}$$

#89185 - $15.00 USD Received 27 Nov 2007; revised 31 Dec 2007; accepted 4 Jan 2008; published 11 Jan 2008

It is clear that Eqn. (14) can be used to produce the maximum values of energy intensity. Assume $E_0 = 1$ and the intensity of the nth order of the scattered field can be expressed as

$$I_{sn} = 2|H_n^{(1)}(k_1\rho)|^2. \tag{15}$$

It is apparent that as n increases, we will have increased bigger values of I_{sn}. Also for a smaller $k_1\rho$, we can also get a bigger I_{sn}. The maximum value of I_{sn} occurs when $\rho = b$. We can see that as ρ becomes bigger, the I_{sn} values decrease rapidly. Analytically, the total cross section at resonances is approximately given by

$$\sigma_{\text{total}} = \frac{8}{k_1}. \tag{16}$$

For the resonances which are excited by TE wave and produced by the permittivities, the analysis and characteristics are very similar, so details will not be discussed here.

6. Conclusion

We have discussed, in detail, the resonance properties of a coated cylinder illuminated by TM and TE plane waves. The resonances are discussed for different parameters and cases assumed, where the near-field energy distributions have been specifically considered and shown. The peak values of the scattered energy distributions are clearly observed and mathematically described. The related formulas of cross sections in closed form at different surface modes are derived, although the later numerical calculations are only focused on the first order mode at $n = 1$. The results obtained here to enhance the scattered energy in near-field region are important and useful for the optical sensors and imaging.

Acknowledgments

The authors are grateful to the supports in part by US Air Force Office of Scientific Research (AFOSR) Projects (Numbered: AOARD-064031 and AOARD-074024), by a research grant of Academic Research Funds by the Ministry of Education, Singapore via National University of Singapore, and by the Swiss Federal Institute of Technology (EPFL), Lausanne, Switzerland.

#89185 - $15.00 USD Received 27 Nov 2007; revised 31 Dec 2007; accepted 4 Jan 2008; published 11 Jan 2008